A Batch-Incremental Video Background Estimation Model using Weighted Low-Rank Approximation of Matrices

Aritra Dutta
KAUST, KSA
aritra.dutta@kaust.edu.sa

Xin Li
UCF, USA
xin.li@ucf.edu

Peter Richtárik
KAUST, University of Edinburgh
peter.richtarik@kaust.edu.sa

Abstract

Principal component pursuit (PCP) is a state-of-the-art approach to background estimation problems. Due to their higher computational cost, PCP algorithms, such as robust principal component analysis (RPCA) and its variants, are not feasible in processing high definition videos. To avoid the curse of dimensionality in those algorithms, several methods have been proposed to solve the background estimation problem incrementally. We build a batch-incremental background estimation model by using a special weighted low-rank approximation of matrices. Through experiments with real and synthetic video sequences, we demonstrate that our model is superior to the existing state-of-the-art background estimation algorithms such as GRASTA, ReProCS, incPCP, and GFL.

1. Introduction

Background estimation and moving object detection are two important steps in many computer vision systems and video-surveillance applications. In the past decade, one of the prevalent approaches used for background estimation treats it as a low-rank and sparse matrix decomposition problem [1, 3, 22, 29]. Oliver *et al*. [24] showed that when the camera motion is small, the background is not expected to change much throughout the video frames, and they assumed it to be low-rank. The seminal work of Lin *et al*., Wright *et al*., and Candès *et al*. [6, 21, 34], which is considered robust principal component analysis (RPCA), solves the problem of background estimation and moving object detection in a single framework. Given a sequence of n video frames with each frame $\mathbf{a}_i \in \mathbb{R}^m$ being vectorized, let the data matrix $A = (\mathbf{a}_1, \mathbf{a}_2, \cdots, \mathbf{a}_n) \in \mathbb{R}^{m\times n}$ be the concatenation of all the video frames. The foreground is usually sparse if its size is relatively small compared to the frame size [6, 21, 34]. Therefore, one can naturally consider a matrix decomposition problem by writing A as the sum of its background and foreground:

$$A = B + F,$$

where $B, F \in \mathbb{R}^{m\times n}$ are the low-rank background and sparse foreground matrices, respectively. Therefore, RPCA solves:

$$\min_B \|A - B\|_{\ell_1} + \lambda\|B\|_*, \tag{1}$$

where $\|\cdot\|_{\ell_1}$ and $\|\cdot\|_*$ denote the ℓ_1 norm and the nuclear norm (sum of the singular values) of matrices, respectively, and $\lambda > 0$ is a balancing parameter.

In contrast, consider a situation when a few, say k, principal directions are already specified and one wants to find a rank r approximation of the data, where $k \le r$. In 1987, Golub *et al*. [13] formulated the following constrained low-rank approximation problem (to be referred as GHS from now on) to address this situation: Given $A = (A_1\ A_2) \in \mathbb{R}^{m\times n}$ with $A_1 \in \mathbb{R}^{m\times k}$ and $A_2 \in \mathbb{R}^{m\times(n-k)}$, find $A_G = (\tilde{B}_1\ \tilde{B}_2)$ such that

$$(\tilde{B}_1\ \tilde{B}_2) = \arg\min_{\substack{B=(B_1\ B_2)\\ B_1=A_1\\ \mathrm{rank}(B)\le r}} \|A - B\|_F^2, \tag{2}$$

where $\|\cdot\|_F$ denotes the Frobenius norm of matrices. That is, Golub *et al*. required a few columns, A_1, of A be preserved to find a low rank approximation of $(A_1\ \ A_2)$. When $A_1 = \emptyset$, we are back to the standard problem of low-rank approximation: find $\tilde{B}$ such that

$$\tilde{B} = \arg\min_{\substack{B\\ \mathrm{rank}(B)\le r}} \|A - B\|_F^2. \tag{3}$$

As it is well known, this problem is equivalent to principal component analysis (PCA) [18] and has a closed form solution that uses the singular value decomposition (SVD) of A: if $A = PDQ^t$ is a SVD of A with unitary matrices P, Q and diagonal matrix D (of non-ascending diagonal entries), then the solution to (3) is given by $\tilde{B} = H_r(A) := PD_rQ^t$, where D_r is a diagonal matrix obtained from D by only keeping the r largest entries and replacing the rest by 0. The operator H_r is referred to as the hard thresholding operator. Using the thresholding operator, GHS problem (2) has a closed form solution as the following theorem explains.

Theorem 1 *[13] Assume* $\mathrm{rank}(A_1) = k$ *and* $r \ge k$*, the solution* $\tilde{B}_2$ *in (2) is given by*

$$\tilde{B}_2 = P_{A_1}(A_2) + H_{r-k}\left(P_{A_1}^{\perp}(A_2)\right), \quad (4)$$

where P_{A_1} and $P_{A_1}^{\perp}$ are the projection operators to the column space of A_1 and its orthogonal complement, respectively.

If we assume that some pure background frames are known, we can apply GHS by using these background frames as the first block matrix A_1. Similarly, recently, Xin *et al.* [35] proposed a *supervised* learning model called generalized fused Lasso (GFL) which solves:

$$\min_{\substack{B \\ B=(B_1\ B_2) \\ B_1=A_1}} \quad \text{rank}(B) + \|A - B\|_{gfl}, \quad (5)$$

where $\|\cdot\|_{gfl}$ denotes a norm that is a combination of the ℓ_1 norm and a local spatial total variation norm (to encourage connectivity of the foreground). To solve GFL problem (5), Xin *et al.* [35] further specialized the above model by requiring $\text{rank}(B) = \text{rank}(A_1)$. Note that, with this specialization, problem (5) can be viewed as a constrained low-rank approximation problem as in GHS problem (2), and it can be formulated as follows:

$$\min_{\substack{B=(B_1\ B_2) \\ \text{rank}(B)\leq r \\ B_1=A_1}} \|A - B\|_{gfl}. \quad (6)$$

1.1. Incremental Methods

Conventional PCA [18] is an essential tool to numerically solve both RPCA and GFL problems. PCA operates at a cost of $\min\{\mathcal{O}(m^2n), \mathcal{O}(mn^2)\}$, which is due to the SVD of an $m \times n$ data matrix. For RPCA algorithms, the space complexity of an SVD computation is approximately $\mathcal{O}((m+n)r)$, where r is the rank of the low-rank approximation matrix in each iteration, which is increasing. And a high resolution video sequence characterized by very large m, is computationally extremely expensive for the RPCA and GFL algorithms. For example, the accelerated proximal gradient (APG) algorithm runs out of memory to process 600 video frames each of size 300×400 on a computer with 3.1 GHz Intel Core i7-4770S processor and 8GB memory. In the past few decades, incremental PCA (IPCA) was developed for machine learning applications to reduce the computational complexity of performing PCA on a huge data set. The idea is to produce an efficient SVD calculation of an augmented matrix of the form $[A\ \tilde{A}]$ by using the SVD of A, where $A \in \mathbb{R}^{m\times n}$ is the original matrix and $\tilde{A}$ contains r newly added columns [37]. Similar to the IPCA, several methods have been proposed to solve the background estimation problem in an incremental manner [12, 20]. In 2012, He *et al.* [16] proposed the Grassmannian robust adaptive subspace estimation (GRASTA), a robust subspace tracking algorithm and showed its application in background estimation problems. More recently, Guo *et al.* [14] proposed another online algorithm for separating sparse and low dimensional subspace. For initial sequence of training background video frames, Guo *et al.* devised a recursive projected compressive sensing algorithm (ReProCS) for background estimation (see also [15, 25]). Following a modified framework of the conventional RPCA problem, Rodriguez *et al.* [28] formulated the incremental principal component pursuit (incPCP) algorithm which processes one frame at a time incrementally and uses only a few frames for initialization of the prior (see also [26, 27]). To the best of our knowledge, these are the state-of-the-art incremental background estimation models.[1]

1.2. Contributions

In this paper, we propose an adaptive batch-incremental model for background estimation. Our model finds the background frame indexes robustly and incrementally to process the entire video sequence. Unlike the models described previously, we do not require any training frames. The model we use allows us to use the background information from previous batch in a naturally.

Before describing our model, let us revisit the idea of Golub *et al.* Inspired by (2) and by applications in which A_1 may contain noise, we require $\|A_1 - B_1\|_F$ small not $B_1 = A_1$ as in (2). This leads Dutta *et al.* [9, 10, 11] to consider the following more general weighted low-rank (WLR) approximation problem:

$$\min_{\substack{X=(X_1\ X_2) \\ \text{rank}(X)\leq r}} \|\left((A_1\ A_2) - (X_1\ X_2)\right) \odot W\|_F^2, \quad (7)$$

where $W \in \mathbb{R}^{m\times n}$ is a matrix with non-negative entires and $\odot$ denotes the Hadamard product. Using $W = (W_1\ \ \mathbb{1})$, Dutta *et al.* [9, 11] applied (7) to solve background estimation problems. Here we propose a batch-incremental background estimation model, using the WLR algorithm of Dutta *et al.* to gain robustness. Similar to the ℓ_1 norm used in conventional and in the incremental methods, a weighted Frobenius norm used in [9, 11] to make WLR robust to the outliers for background estimation problems [9, 11]. Our batch model is as fast as incPCP and ReProCS also, our model can deal with high quality video sequences as well as incPCP and ReProCS. Some conventional algorithms, such as supervised GFL or ReProCS require an initial training sequence, which does not contain any foreground object. Our experimental results for both synthetic and real video sequences show that unlike the supervised GFL and ReProCS, our model does not require a prior; instead, it can estimate its own prior robustly from the entire data. We believe the adaptive nature of this algorithm is well suited for real time high-definition video surveillance and for panning motions of the camera where the background slowly evolves.

[1] We refer the readers to [17, 30].

Algorithm 1: WLR Algorithm

Input : $A = (A_1 \;\; A_2) \in \mathbb{R}^{m\times n}$ (the data matrix), $W = (W_1 \;\; \mathbb{1}) \in \mathbb{R}^{m\times n}$ (the weight), threshold $\epsilon > 0$;
Initialize: $(X_1)_0, C_0, B_0, D_0$;
while *not converged* **do**
  $E_p = A_1 \odot W_1 \odot W_1 + (A_2 - B_p D_p) C_p^T$;
  for $i = 1 : m$ **do**
    $(X_1(i,:))_{p+1} = (E(i,:))_p (\text{diag}(W_1^2(i,1)\; W_1^2(i,2) \cdots W_1^2(i,k)) + C_p C_p^T)^{-1}$;
  end
  $C_{p+1} = ((X_1)_{p+1}^T (X_1)_{p+1})^{-1} (X_1)_{p+1}^T (A_2 - B_p D_p)$;
  $B_{p+1} = (A_2 - (X_1)_{p+1} C_{p+1}) D_p^T (D_p D_p^T)^{-1}$;
  $D_{p+1} = (B_{p+1}^T B_{p+1})^{-1} B_{p+1}^T (A_2 - (X_1)_{p+1} C_{p+1})$;
  $p = p + 1$;
end
Output : $(X_1)_{p+1}, (X_1)_{p+1} C_{p+1} + B_{p+1} D_{p+1}$.

Algorithm 2: Incremental Background Estimation using WLR (inWLR)

1 **Input** : p, $A = (A^{(1)} \;\; A^{(2)} \ldots A^{(p)}) \in \mathbb{R}^{m\times n}$, $\tau > 0$ (for SVT), $\alpha, \beta > 0$ (for weights), threshold $\epsilon > 0$, $k_{max},\; i_r \in \mathbb{N}$;
2 Run SVT on $A^{(1)}$ with parameter τ to obtain: $A^{(1)} = B_{In}^{(1)} + F_{In}^{(1)}$;
3 Initialize the background block by $B = B_{In}^{(1)}$ and $A^{(0)} = A^{(1)}$;
4 **for** $j = 1 : p$ **do**
5   Identify the indices S of at most k_{max} columns of $A^{(j-1)}$ that are closest to background using B and $F = A^{(j-1)} - B$;
6   Set $k = \#(S), r = k + i_r$;
7   Set the first block: $\tilde{A}_1 = (A^{(j-1)}(:,i))_{m\times k}$ with $i \in S$;
8   Define $W = (W_1 \;\; \mathbb{1})$ with $W_1 \in \mathbb{R}^{m\times k}$ where $(W_1)_{ij}$ are randomly chosen from $[\alpha, \beta]$;
9   Apply **Algorithm 1** on $\tilde{A}^{(j)} = (\tilde{A}_1 \;\; A^{(j)})$ using threshold ϵ and weight W to obtain its low rank component $\tilde{B}^{(j)}$ and define $\tilde{F}^{(j)} = \tilde{A}^{(j)} - \tilde{B}^{(j)}$;
10   Take the sub-matrix of $\tilde{B}^{(j)}$ corresponding to the $A^{(j)}$ block such that $A^{(j)} = B^{(j)} + F^{(j)}$;
11   Update the background block: $B = \tilde{B}^{(j)}$;
end
12 **Output** : $B = (B^{(1)}, B^{(2)}, ..., B^{(p)})$.

1.3. The WLR algorithm

We now briefly overview the WLR algorithm proposed by Dutta *et al.* [7, 10, 11]. Let $\text{rank}(X_1) = k$. Then any X_2 such that $\text{rank}(X_1 \;\; X_2) \leq r$ can be given in the form,

$$X_2 = X_1 C + BD,$$

for some matrices $B \in \mathbb{R}^{m\times(r-k)}$, $D \in \mathbb{R}^{(r-k)\times(n-k)}$, and for $C \in \mathbb{R}^{k\times(n-k)}$. Therefore, problem (7) with $W = (W_1 \;\; \mathbb{1})$ of compatible block partition is reduced to:

$$\min_{X_1,C,B,D} \|(A_1 - X_1) \odot W_1\|_F^2 + \|A_2 - X_1 C - BD\|_F^2. \tag{8}$$

The complexity of one iteration of Algorithm 1 is $\mathcal{O}(mk^3 + mnr)$ [10].

2. An incremental model using WLR

In this section, we propose an incremental weighted low-rank approximation (inWLR) algorithm for background estimation based on WLR (see Algorithm 2 and Figure 1). Our algorithm fully exploits WLR, in which a prior knowledge of the background space can be used as an additional constraint to obtain the low rank (thus the background) estimation of the data matrix A. First, we partition the original video sequence into p batches: $A = (A^{(1)} \;\; A^{(2)} \ldots A^{(p)})$, where the batch sizes do not need to be equal. Instead of working on the entire video sequence, the algorithm incrementally works through each batch. To initialize, the algorithm coarsely estimates the possible background frame indices of $A^{(1)}$: we run the classic singular value thresholding (SVT) of Cai *et al.* [5] on $A^{(1)}$ to obtain a low rank component (containing the estimations of the background frames) $B_{In}^{(1)}$ and let $F_{In}^{(1)} = A^{(1)} - B_{In}^{(1)}$ be the estimation of the foreground matrix (Step 2). From the above estimates, we obtain the initialization for B and $A^{(0)}$ (Step 3). Then, we go through each batch $A^{(j)}$, using the estimates of the background from the previous batch as prior for the WLR algorithm to obtain the background $\tilde{B}^{(j)}$ (Step 9). To determine the indices of the frames that contain the least information of the foreground we identify the "best background frames" by using a modified version of the percentage score model by Dutta *et al.* [8] (Step 5). Using this modified model allows us to estimate k, r, and the first block $\tilde{A}_1$ which contains the background prior knowledge (Steps 6-7). Weight matrix $W = (W_1 \;\; \mathbb{1})$ is chosen by randomly picking the entries of the first block W_1 from an interval $[\alpha, \beta]$ by using an uniform distribution, where $\beta > \alpha > 0$ are large (Step 8). To understand the effect of using a large weight in W_1, we refer the reader to [9, 10]. Finally, we collect background information for next iteration (Steps 10-11). Note that the number of columns of the weight matrix W_1 is k, which is controlled by bound k_{max} so that the column size of $\tilde{A}^{(j)}$ does not grow with j. The output of the algorithm is the background estimations for each batch collected in a single matrix B. When the camera motion is small, updating the first block matrix $\tilde{A}_1$ (Step 7) has trivial impact on the model since it does not change much. However, when the camera is panning and the background is continuously evolving, our inWLR could be proven very robust as new frames are entering in

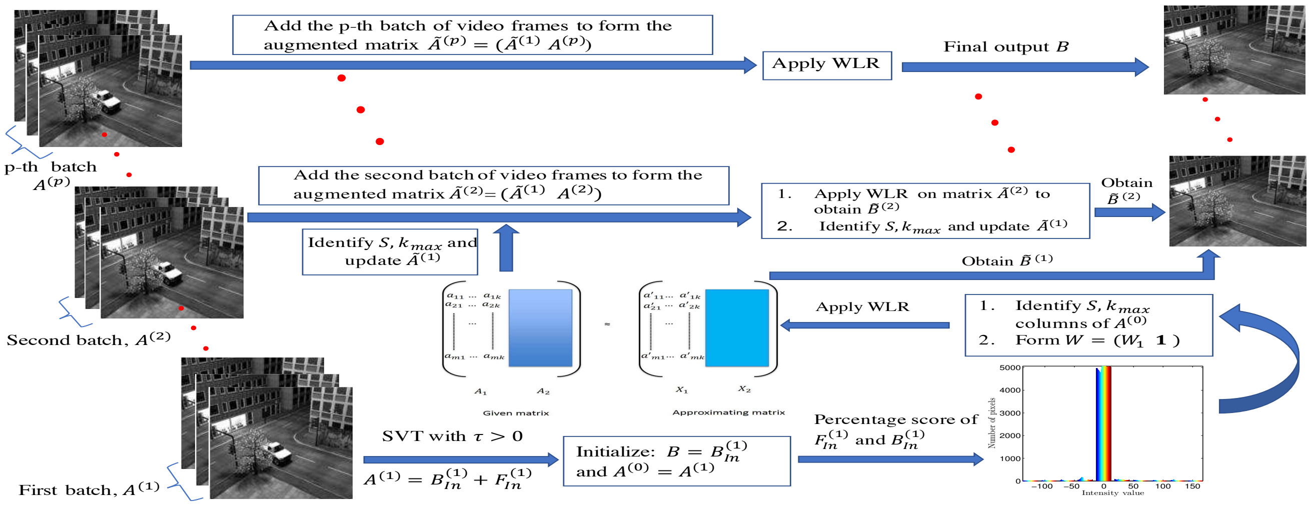

Figure 1: A flowchart for WLR inspired background estimation model proposed in Algorithm 2.

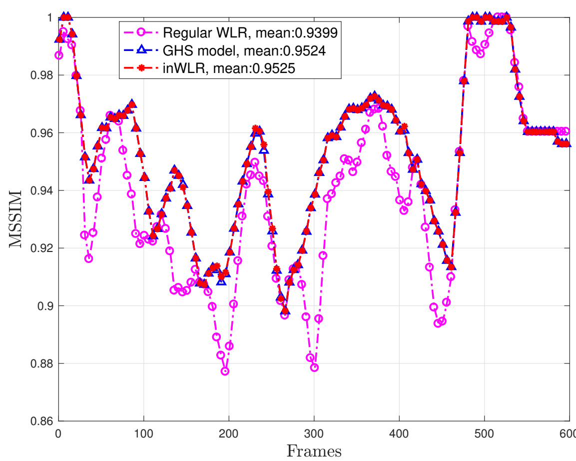

Figure 2: Comparison of MSSIM of WLR acting on all frames, inWLR, and GHS inspired background estimation model with frame size $[144, 176]$ and $p = 6$.

the video.

2.1. Complexity analysis

Now, we analyze the complexity of Algorithm 2 for equal batch size. Primarily, the cost of the SVT algorithm in Step 2 is only $\mathcal{O}(\frac{mn^2}{p^2})$. Next, in Step 9, the complexity of implementing Algorithm 1 is $\mathcal{O}(mk^3 + \frac{mnr}{p})$. Note that r and k are linearly related and $k \leq k_{max}$. Once we obtain a refined estimate of the background frame indices S as in Step 5 and form an augmented matrix by adding the next batch of video frames, a very natural question in proposing our WLR inspired Algorithm 2 is: why do we use Algorithm 1 in each incremental step (Step 9) of Algorithm 2 instead of using a closed form solution (4) of GHS? We justify as follows: the estimated background frames $\tilde{A}_1$ are not necessarily exact background; they are only estimations of background. Thus, GHS inspired model may be forced to follow the wrong data while inWLR allows enough flexibility to find the best fit to the background subspace. This is confirmed by our numerical experiments (see Section 3.1 and Figure 2). Thus, to analyze the entire sequence in p batches, the complexity of Algorithm 2 is approximately $\mathcal{O}(m(k^3p + nr))$. Note that the complexity of Algorithm 2 is dependent on the partition p of the original data matrix. Our numerical experiments suggest that for video frames of varying sizes, the choice of p plays an important role and is empirically determined.

Unlike Algorithm 2, if Algorithm 1 is used on the entire data set and if the number of possible background frame indices is k', then the complexity is $\mathcal{O}(mk'^3 + mnk')$. When k' grows with n and becomes much bigger than k_{max} in order to achieve competitive performance, we see that Algorithm 1 tends to slow down with higher overhead than Algorithm 2 does (see Table 1).

3. Qualitative and quantitative analysis

Due to the availability of ground truth frames for each foreground mask, we use 600 frames of the *Basic* scenario of the Stuttgart artificial video sequence [4] to analyze them quantitatively and qualitatively. To capture an unified comparison against each method, we resize the video frames to [144,176] and for inWLR set $p = 6$; that is, we add a batch of 100 new video frames in every iteration until all frames are exhausted.

3.1. Comparison with GHS

Because the *Basic* scenario has no noise, once we estimate the background frames, GHS can be used as a baseline

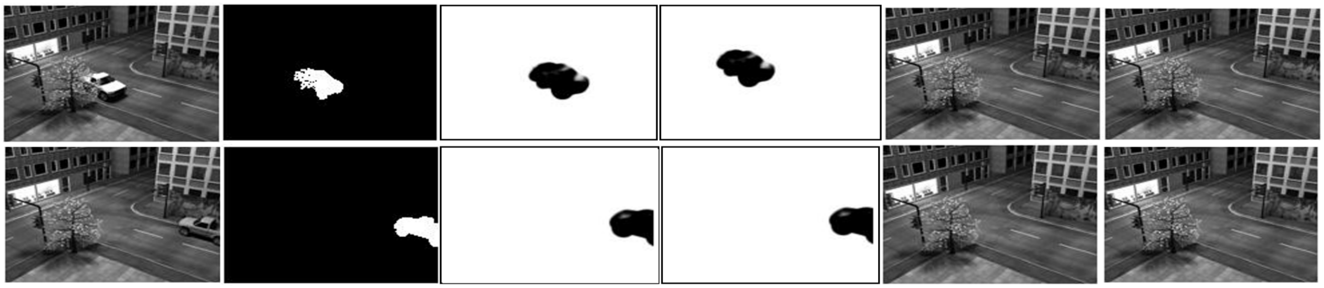

Figure 3: SSIM map of inWLR and GHS inspired background estimation model, frame size $[144, 176]$, and $p = 6$. Top to bottom: Frame 420 with dynamic foreground, frame 600 with static foreground. Left to right: Original, ground truth, inWLR SSIM, GHS SSIM, inWLR background, and GHS background. SSIM index of the methods are 0.95027 and 0.96152, respectively.

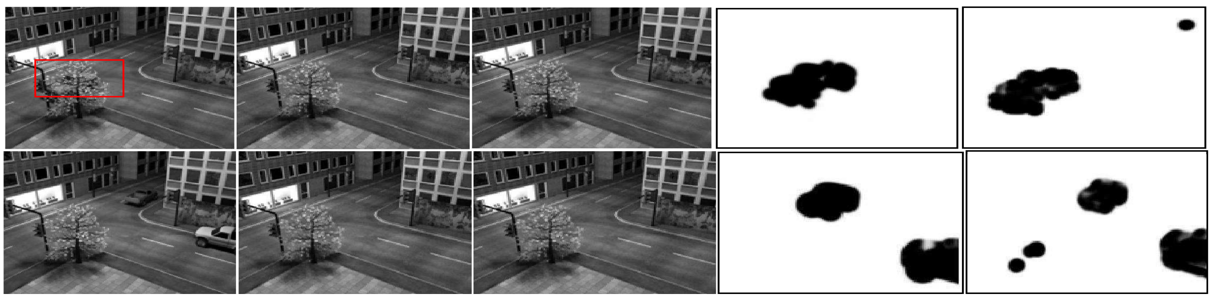

Figure 4: *Basic* scenario frame: (a) 50, (b)100. Left to right: Original, inWLR background, GFL background, inWLR SSIM, and GFL SSIM. The MSSIM of inWLR on two frames are 0.9595 and 0.9457, and that of GFL are 0.9534 and 0.9443, respectively.

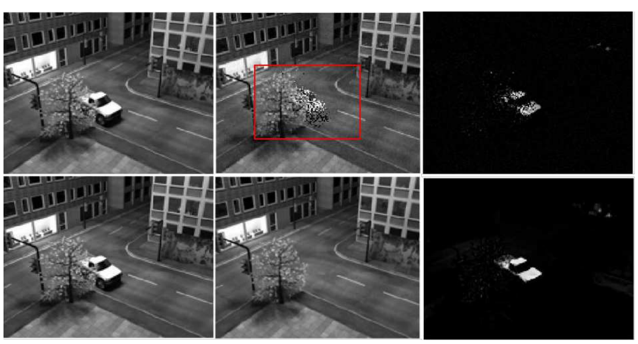

Figure 5: *Basic* scenario frame 420: (a) GRASTA, (b) inWLR. Left to right: Original, background, and foreground. GRASTA with subsample rate 10% recovers a fragmentary foreground and degraded background.

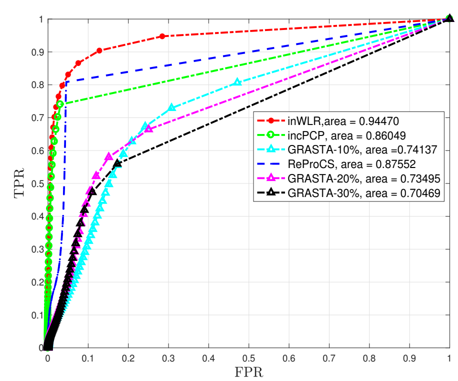

Figure 6: ROC curves on Stuttgart *Basic* scenario to compare between GRASTA, inWLR, incPCP, and ReProCS.

method in comparing the effectiveness of Algorithm 2. To demonstrate the benefit of using an iterative process as in Algorithm 1, we first compare the performance of Algorithm 2 against the GHS inspired models. We also compare regular WLR acting on all 600 frames with the parameters specified in [11]. The structural similarity index (MSSIM) is used to quantitatively evaluate the overall image quality as it mostly agrees with the human visual perception [32]. To calculate the MSSIM of each recovered foreground video frame, we consider a 11×11 Gaussian window with standard deviation (σ) 1.5. We perceive the information of how the high-intensity regions of the images come through the noise, and consequently, we pay much less attention to the low-intensity regions. We remove the noisy components

Figure 7: *Basic* scenario frame 123. Left to right: Original, inWLR background, ReProCS background, inWLR foreground, ReProCS foreground, and ground truth. Both methods recover similar quality background, however, ReProCS foreground has more false positives than inWLR.

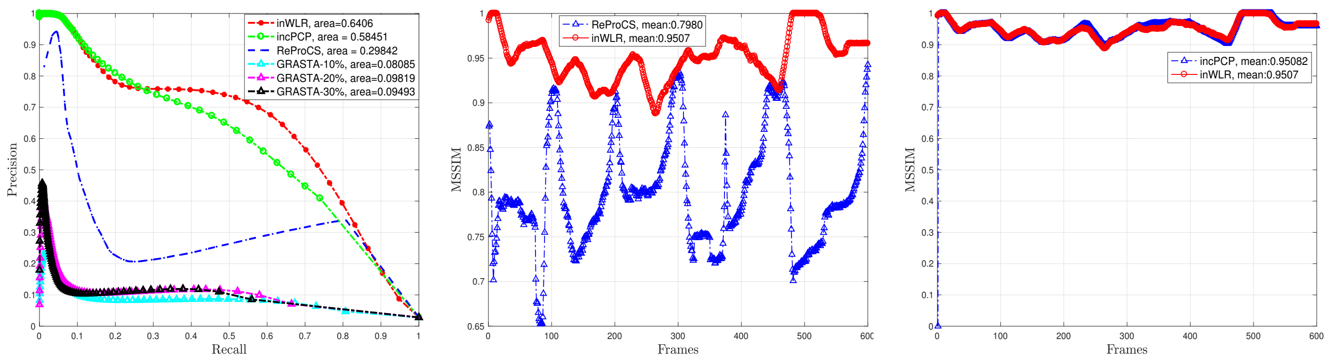

(a) (b) (c)

Figure 8: (a) Precision-Recall curves on Stuttgart *Basic* scenario to compare between ReProCS, inWLR, and GRASTA. MSSIM on Stuttgart *Basic* scenario to compare between: (b) ReProCS and inWLR, (c) incPCP and inWLR.

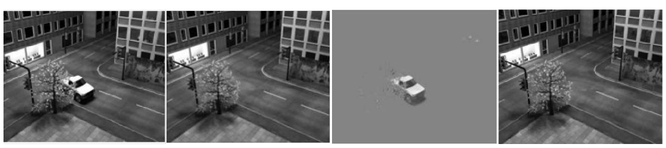

Figure 9: *Basic* scenario frame 420. Left to right: Original, incPCP background, incPCP foreground, and inWLR background. Both methods work equally well in detecting the dynamic foreground object.

from the foreground recovered by inWLR, F by using a threshold ϵ_1 (calculated implicitly in Step 5 of Algorithm 2 to choose the background frames, see [8]), such that we set the components below ϵ_1 in F to 0. The average computation time of inWLR is approximately in the range 17.829035 seconds to 19.5755 seconds in processing 600 frames each of size 144×176. On the other hand, the GHS inspired model and WLR model take approximately 273.8382 and 64.5 seconds, respectively. The MSSIM presented in Figure 2 indicates that the inWLR and GHS inspired model produce the same result, with inWLR being more time efficient than GHS. Next in Figure 3, the SSIM map of two sample video frames of the *Basic* scenario show that both methods recover the similar quality background and foreground frames. Figure 2 shows that to work on a high resolution video, inWLR is more accurate than GHS and WLR.

3.2. Comparison with GFL

We compare the performance of inWLR with the GFL model of Xin *et al.* [35][2]. For both models, we use 200 frames of the *Basic* sequence, each frame resized to $[144, 176]$. The background recovered and the SSIM map in Figures 4 and 11 show that both methods are very competitive. However, it is worth mentioning that inWLR is extraordinarily time efficient compare with the GFL model.

3.3. Comparison with other state-of-the-art models

In this section, we compare the performance of inWLR against other incremental background estimation models such as GRASTA, incPCP, and ReProCS on 600 frames of the *Basic* scenario of the Stuttgart sequence. For quantitative measure, we use the receiver operating characteristic (ROC) curve, the recall and precision (RP) curve, and the MSSIM. For ROC curve and RP curve, we use a uniform threshold vector $\mathrm{linspace}(0, 255, 100)$ to compare pixel-wise predictive analysis between each recovered foreground

[2]http://idm.pku.edu.cn/staff/wangyizhou/

Figure 10: *Basic* scenario frame 600. Left to right: Original, incPCP background, incPCP foreground, inWLR background, inWLR SSIM, and incPCP SSIM. incPCP fails to detect the static foreground object, though a careful reader can detect a blurry reconstruction of the car in incPCP foreground. However, the SSIM map of both methods are equally good.

Dataset	ReProCS	GRASTA	inWLR	incPCP	WLR	GHS
Basic	15.8122	22.39	17.829035	58.4132	64.0485	273.8382
Fountain	-	-	3.709931	-	7.135779	4.327475
Waving Tree	4.548824	-	3.3873	-	13.751490	42.302412

Table 1: Computational time comparison. All experiments were performed on a computer with 2.7 GHz Intel Core i7 processor and 16 GB memory. The best and the 2^{nd} best results are colored with red and blue, respectively. For frame numbers, frame size, and p for inWLR see Section 3 and 4.

frame and the corresponding ground truth frame.

3.3.1 Comparison with GRASTA [16]

At each time step i, GRASTA solves the following optimization problem: For a given orthonormal basis $U_{\Omega_s} \in \mathbb{R}^{|\Omega_s| \times d}$ solve

$$\min_x \|U_{\Omega_s} x - A_{\Omega_s}(:, i)\|_{\ell_1}, \tag{9}$$

where each video frame $A(:, i) \in \mathbb{R}^m$ is subsampled over the index set $\Omega_s \subset \{1, 2, \cdots, m\}$ following the model: $A_{\Omega_s}(:, i) = U_{\Omega_s} x + F_{\Omega_s}(:, i) + \epsilon_{\Omega_s}$, such that, $x \in \mathbb{R}^d$ is a weight vector and $\epsilon_{\Omega_s} \in \mathbb{R}^{|\Omega_s|}$ is a Gaussian noise vector. After updating x, one has to update U_{Ω_s}. We set the subsample percentage s at 0%, 10%, 20%, and at 30% respectively, estimated rank 60, and keep the other parameters the same as those in [16]. The GRASTA code is obtained from the author's website.[3] Note that for a lower estimated rank GRASTA does not perform well in *Basic* scenario. Referring the qualitative result in Figure 5, we only provide the ROC curve and RP curve to compare GRASTA with different subsamples s and inWLR (see Figure 6 and 8a). The ROC curves and RP curves show the superior performance of inWLR on the Stuttgart *Basic* scenario.

3.3.2 Comparison with ReProCS [14]

ReProCS is a two stage algorithm. In the first stage, given a sequence of training background frames, say t, the algorithm finds an approximate basis which is ideally of low-rank. After estimating the initial low-rank subspace in the second stage, the algorithm recursively estimates F_{t+1}, B_{t+1} and the subspace in which B_{t+1} lies. We use 200 background frames of the *Basic* sequence for initialization of ReProCS. Figure 7 shows that both methods recover similar quality background. However, ReProCS foreground contains more false positives than inWLR foreground. The ROC curve, RP curve, and MSSIM in Figure 6, 8a, and 8b support our claim quantitatively for the *Basic* sequence. Although the average computation time for ReProCS is 15.644460 seconds, which is better than inWLR.

3.3.3 Comparison with incPCP [28]

incPCP follows a modified framework of PCP but is built with the assumption that the partial rank r SVD of first $k-1$ background frames B_{k-1} is known. And using them, A_{k-1} can be written as $A_{k-1} = B_{k-1} + F_{k-1}$. Therefore, for a new video frame $A(:, k)$, one can solve the optimization problem as follows:

$$\min_{\substack{B_k, F_k \\ \operatorname{rank}(B_k) \le r}} \|B_k + F_k - A_k\|_F^2 + \lambda \|F_k\|_{\ell_1},$$

where $A_k = [A_{k-1} \;\; A(:, k)]$ and $B_k = [U_r \Sigma_r V_r^T \;\; B(:, k)]$ such that $U_r \Sigma_r V_r^T$ is a partial SVD of B_{k-1}. According to [28], the initialization step can be performed incrementally. For the Stuttgart sequence, the algorithm uses the first video frame for initialization. The incPCP code is downloaded from the author's website[4]. From the MSSIM presented in Figure 8c and the background recovered by both methods in Figure 9, both methods appear to perform equally well on the *Basic* scenario. However, when the foreground is static (as in frames 551-600 of the Stuttgart se-

[3] https://sites.google.com/site/hejunzz/grasta

[4] https://sites.google.com/a/istec.net/prodrig/Home/en/pubs/incpcp

Figure 11: *Waving Tree* frame 247, frame size [120,160]. Left to right: Original, inWLR background ($p = 6$), GFL background, ReProCS background, inWLR SSIM (MSSIM: 0.9592), GFL SSIM (MSSIM: 0.9996), and ReProCS SSIM (MSSIM: 0.5221). inWLR and GFL recover superior quality background.

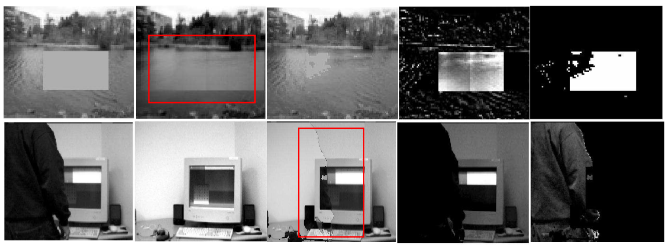

Figure 12: Left to right: Original, inWLR background, ReProCS background, inWLR foreground, and ReProCS foreground. In *Lake* sequence ReProCS performs better, and in *Person* sequence inWLR has better performance.

Figure 13: Top to bottom: *Fountain* 500 frames with $p = 5$, *Campus* 600 frames with $p = 6$, frame size [64,80]. Left to right: Original, inWLR background, and inWLR foreground.

quence), the ℓ_1 norm in incPCP cannot capture the foreground object, thus resulting in the presence of the static car as a part of the background (see Figure 10). On the other hand, our inWLR successfully detects and removes the static foreground from the background.

4. Results on real world sequences

To further validate the robustness of inWLR, we tested it on some challenging real world video sequences containing occlusion, dynamic background, and static foreground. We use I2R and SBI dataset [19, 23, 31] for this purpose. In Figure 11, we compare inWLR against GFL and ReProCS on 60 frames of *Waving Tree* sequence. ReProCS and GFL use 220 and 200 pure background frames respectively as training data. In Figure 12, we compare inWLR against ReProCS on two complex sequences: 80 frames of *Lake*, frame size $[72, 90]$, and, 50 frames of *Person*, frame size $[120, 160]$. In those sequences, for inWLR, we set $p = 8$ and 5, respectively. Due to the absence of ground truth we only provide qualitative comparison. In Figure 13, we demonstrate the performance of inWLR on two data sets with dynamic background and semi-static foreground. In almost every video sequence, inWLR performs reasonably well. See Table 1 for the comparisons between computational time. Due to space limitation we only provide quantitative result for six sequences of the SBI dataset (see Table 2). For this purpose, we use two additional metrics: multi-scale SSIM (MSSSIM) [33] and color image quality measure (CQM) [2, 36][5]. For the SBI dataset, we use a Gaussian window of size 9×9 and standard deviation (σ) 1.5 to calculate MSSSIM.

Dataset	MSSIM	MSSSIM[33]	CQM[36]
IBMtest2	0.99979	0.99998	76.30844
Foliage	0.9865	0.99803	85.92427
Candela	0.9999	0.9999949	79.17169
Caviar2	0.99998	0.99999	78.00402
HallMonitor	0.99993	0.99998	63.78041
Snellen	0.99179	0.99891	90.08299

Table 2: Performance of inWLR on SBI dataset [23]. Frame size 144×176.

5. Conclusion

In this paper we proposed a novel model for background estimation. Our model operates on the entire data in a batch-incremental way and adaptively determines the background frames without requiring any prior estimate. Furthermore, our model does not require much storage and allows slow changes in the background. Our extensive qualitative and quantitative comparison on real and synthetic video sequences demonstrate the robustness of our model. The batch sizes and the parameters in our model are still empirically selected. Therefore, we plan to propose a more robust estimate of the parameters and explore the possibilities that our algorithm can handle videos of more dynamic background.

[5]The MATLAB codes for MSSSIM and CQM are downloaded from http://sbmi2015.na.icar.cnr.it/SBIdataset.html

References

[1] T. Bouwmans. Traditional and recent approaches in background modeling for foreground detection: An overview. *Computer Science Review*, 11:31 – 66, 2014. 1

[2] T. Bouwmans, L. Maddalena, and A. Petrosino. Scene background initialization: A taxonomy. *Pattern Recognition Letters*, 2017. 8

[3] T. Bouwmans, A. Sobral, S. Javed, S. K. Jung, and E.-H. Zahzah. Decomposition into low-rank plus additive matrices for background/-foreground separation: A review for a comparative evaluation with a large-scale dataset. *Computer Science Review*, 23:1–71, 2017. 1

[4] S. Brutzer, B. Höferlin, and G. Heidemann. Evaluation of background subtraction techniques for video surveillance. *IEEE Computer Vision and Pattern Recognition*, pages 1568–1575, 2012. 4

[5] J. F. Cai, E. J. Candès, and Z. Shen. A singular value thresholding algorithm for matrix completion. *SIAM Journal on Optimization*, 20(4):1956–1982, 2010. 3

[6] E. J. Candès, X. Li, Y. Ma, and J. Wright. Robust principal component analysis? *Journal of the Association for Computing Machinery*, 58(3):11:1–11:37, 2011. 1

[7] A. Dutta. Weighted low-rank approximation of matrices: Some analytical and numerical aspects, 2016. Ph.D. dissertation, Department of Mathematics, University of Central Florida, Orlando, FL. 3

[8] A. Dutta, B. Gong, X. Li, and M. Shah. Weighted singular value thresholding and its applications to background estimation, 2017. arXiv:1707.00133. 3, 6

[9] A. Dutta and X. Li. A fast algorithm for a weighted low rank approximation. In *IEEE 2017 Fifteenth IAPR International Conference on Machine Vision Applications (MVA)*, pages 93–96, 2017. 2, 3

[10] A. Dutta and X. Li. On a problem of weighted low-rank approximation of matrices. *SIAM Journal on Matrix Analysis and Applications*, 38(2):530–553, 2017. 2, 3

[11] A. Dutta and X. Li. Weighted low rank approximation for background estimation problems. In *IEEE International Conference on Computer Vision Workshops (ICCVW)*, 2017. 2, 3, 5

[12] D. Farcas, C. Marghes, and T. Bouwmans. Background subtraction via incremental maximum margin criterion: a discriminative subspace approach. *Machine Vision and Applications*, 23(6):1083–1101, 2012. 2

[13] G. H. Golub, A. Hoffman, and G. W. Stewart. A generalization of the Eckart-Young-Mirsky matrix approximation theorem. *Linear Algebra and its Applications*, 88(89):317–327, 1987. 1

[14] H. Guo, C. Qiu, and N. Vaswani. An online algorithm for separating sparse and low-dimensional signal sequences from their sum. *IEEE Transactions on Signal Processing*, 62(16):4284–4297, 2014. 2, 7

[15] H. Guo, C. Qiu, and N. Vaswani. Practical REPROCS for separating sparse and low-dimensional signal sequences from their sum-part 1. In *IEEE International Conference on Acoustic, Speech and Signal Processing*, pages 4161–4165, 2014. 2

[16] J. He, L. Balzano, and A. Szlam. Incremental gradient on the grassmannian for online foreground and background separation in subsampled video. *IEEE Computer Vision and Pattern Recognition*, pages 1937–1944, 2012. 2, 7

[17] S. Javed, A. Mahmood, T. Bouwmans, and S. K. Jung. Spatiotemporal low-rank modeling for complex scene background initialization. *IEEE Transactions on Circuits and Systems for Video Technology*, 2016. 2

[18] I. T. Jolliffee. Principal component analysis, 2002. Second edition. 1, 2

[19] L. Li, W. Huang, I.-H. Gu, and Q. Tian. Statistical modeling of complex backgrounds for foreground object detection. *IEEE Transactions on Image Processing*, 13(11):1459–1472, 2004. 8

[20] Y. Li, L. Q. Xu, J. Morphett, and R. Jacobs. An integrated algorithm of incremental and robust pca. In *Proceedings 2003 International Conference on Image Processing*, volume 1, pages I–245–I–248, 2003. 2

[21] Z. Lin, M. Chen, and Y. Ma. The augmented Lagrange multiplier method for exact recovery of corrupted low-rank matrices, 2010. arXiv1009.5055. 1

[22] L. Maddalena and A. Petrosino. Background model initialization for static cameras. In *Background Modeling and Foreground Detection for Video Surveillance*, pages 3–1–3–16. Chapman and Hall/CRC, 2014. 1

[23] L. Maddalena and A. Petrosino. Towards benchmarking scene background initialization. In *New Trends in Image Analysis and Processing – ICIAP 2015 Workshops*, pages 469–476, 2015. 8

[24] N. Oliver, B. Rosario, and A. Pentland. A Bayesian computer vision system for modeling human interactions. In *International Conference on Computer Vision Systems*, pages 255–272, 1999. 1

[25] C. Qiu and N. Vaswani. Support predicted modified-CS for recursive robust principal components pursuit. In *IEEE International Symposium on Information Theory*, pages 668–672, 2011. 2

[26] P. Rodriguez and B. Wohlberg. A matlab implementation of a fast incremental principal component pursuit algorithm for video background modeling. In *IEEE International Conference on Image Processing*, pages 3414–3416, 2014. 2

[27] P. Rodriguez and B. Wohlberg. Translational and rotational jitter invariant incremental principal component pursuit for video background modeling. In *2015 IEEE International Conference on Image Processing*, pages 537–541, 2015. 2

[28] P. Rodriguez and B. Wohlberg. Incremental principal component pursuit for video background modeling. *Journal of Mathematical Imaging and Vision*, 55(1):1–18, 2016. 2, 7

[29] A. Sobral and A. Vacavant. A comprehensive review of background subtraction algorithms evaluated with synthetic and real videos. *Computer Vision and Image Understanding*, 122:4–21, 2014. 1

[30] A. Sobral and E.-H. Zahzah. Matrix and tensor completion algorithms for background model initialization: A comparative evaluation. *Pattern Recognition Letters*, 2016. 2

[31] K. Toyama, J. Krumm, B. Brumitt, and B. Meyers. Wallflower: Principles and practice of background maintainance. *Seventh International Conference on Computer Vision*, pages 255–261, 1999. 8

[32] Z. Wang, A. C. Bovik, H. R. Sheikh, and E. P. Simoncelli. Image quality assessment: from error visibility to structural similarity. *IEEE Transaction on Image Processing*, 13(4):600–612, 2004. 5

[33] Z. Wang, E. P. Simoncelli, and A. C. Bovik. Multi-scale structural similarity for image quality assessment. In *37th IEEE Asilomar Conference on Signals, Systems, and Computers*, pages 1398–1402, 2003. 8

[34] J. Wright, Y. Peng, Y. Ma, A. Ganseh, and S. Rao. Robust principal component analysis: exact recovery of corrputed low-rank matrices by convex optimization. *Proceedings of 22nd Advances in Neural Information Processing systems*, pages 2080–2088, 2009. 1

[35] B. Xin, Y. Tian, Y. Wang, and W. Gao. Background subtraction via generalized fused Lasso foreground modeling. *IEEE Computer Vision and Pattern Recognition*, pages 4676–4684, 2015. 2, 6

[36] Y. Yalman and I. Erturk. A new color image quality measure based on yuv transformation and psnr for human vision system. *Turkish Journal of Electrical Engineering and Computer Sciences*, 21(2):603–612, 2013. 8

[37] H. Zhao, P. C. Yuen, and J. T. Kwok. A novel incremental principal component analysis and its application for face recognition. *IEEE Transactions on Systems, Man, and Cybernetics, Part B: Cybernetics*, 36(4):873–886, 2006. 2